PHYSICAL REVIEW A

ATOMIC, MOLECULAR, AND OPTICAL PHYSICS

THIRD SERIES, VOLUME 47, NUMBER 4 PART B APRIL 1993

ARTICLES

Two-photon coincident emission from thick targets for 70-keV incident electrons

J. Liu, D. L. Kahler, and C. A. Quarles
Texas Christian University, Fort Worth, Texas 76129
(Received 15 June 1992)

Two-photon coincidence yields have been measured in thick targets of C, Al, Ag, and Ta for 70 keV incident electrons and photons radiated at ±45° to the incident beam. A theoretical model, which is more rigorous, has been developed to simulate the two-photon processes of coherent thick-target double bremsstrahlung (TTDB) and the incoherent emission of two single-bremsstrahlung (SBSB) photons in a thick-target environment. The model is based on an integration of the thin-target cross sections over the target thickness taking into account electron energy loss, electron backscattering, and photon attenuation. It predicts a yield that is much lower than that of the previous model. The prediction of the model fits the present experimental data well by adjusting the relative weight of the two competing processes, and we find that TTDB dominates at low Z and incoherent SBSB dominates at higher Z.

PACS number(s): 34.80.Dp, 79.20.Kz

I. INTRODUCTION

Double bremsstrahlung (DB) is a quantum electrodynamic process in which two photons are emitted simultaneously in the inelastic scattering of an electron by the Coulomb field of an atom. The process was introduced in 1934 by Heitler and Nordheim [1] as a radiative correction to the single bremsstrahlung (SB) theory. A measurement of the DB cross section was made in 1985 by Altman and Quarles [2] in a two-photon coincidence experiment for 75-keV electrons incident on thin targets in which photons were detected at ±90° to the incident-beam direction. A cross section quadruply differential in the two-photon energies and angles was measured, and was found to be about two orders of magnitude larger than a theoretical value determined using a numerical evaluation of the relativistic first-order Born approximation formula obtained by Smirnov [3].

A possible explanation of this large discrepancy was a background process in which electrons first elastically scattered in the target into one of the Mylar detector windows, then second, produced thick-target double bremsstrahlung in the Mylar so that one photon was detected in each detector. This was plausible in the 90° geometry since both detectors could see each detector window, and led to a detailed consideration of double bremsstrahlung in a thick target, that is a target thick enough to stop the incident electrons, yet thin enough to transmit a substantial fraction of the radiated photons. Lehtihet and Quarles [4] developed a model of DB in thick targets (TTDB) which was based on an analogy with the treatment of thick-target single bremsstrahlung [5] which predicted a two-photon yield from the Mylar windows consistent with the two-photon cross section measured by Ref. [2].

To test the TTDB model, Lehtihet and Quarles [6] measured the two-photon coincidence yield from 84-keV conversion electrons from a ^{109}Cd radioactive source incident on thick targets of Ag, Au, and Pb. In this experiment a ±45° geometry was utilized and the detectors were shielded from one another in order to avoid any enhancement in the yield from cross-talk between the detectors. The measured rates were found to agree well with the TTDB model of Ref. [4], which further supported the proposed background effect as an explanation for the discrepancy in the thin-target experiment of Ref. [2], and emphasized the need for a geometry in which the two detectors could not see each other.

Recently, Kahler, Liu, and Quarles have measured the DB cross section in *thin* targets of Al, Cu, Ag, Tb, and U for 70-keV incident electrons and a ±45° geometry [7]. This experiment improves the sensitivity of the cross-section measurement by about two orders of magnitude over that of Ref. [2]. In contrast with the earlier work, the results obtained are generally in good agreement with the relativistic first-order Born approximation except for

 ©1993 The American Physical Society

a deviation, which should be expected, from the Z^2 dependence predicted by the first-order Born approximation. It should be stressed that the theory compared with is a numerical integration of the fully differential cross section over the direction of the unobserved electron. The formula integrated [Eq. (3) of Ref. [3]] is complicated, and there has been some question as to its accuracy [8] since the nonrelativistic limit of the equation given by Smirnov is clearly incorrect. However, recently the formula has been checked by Scofield [9] in an independent calculation and found to be correct. While there has been no independent evaluation of the integral of the formula over the unobserved outgoing electron, we have evaluated this in several independent computer programs over the past several years using different numerical integration techniques and found consistent agreement among our calculations. Further theoretical work on the integrated cross section is desirable, however. There is a nonrelativistic Coulomb result now available from Florescu [10]. The prediction of this nonrelativistic calculation is significantly lower than the relativistic calculation for the 45° geometry. A detailed comparison of the two calculations in an energy region where they may be expected to agree is currently underway.

The good agreement obtained in Ref. [7] with the thin-target cross section in our geometry in which cross talk was prevented between the two detectors motivated us to investigate directly the thick-target yield in an accelerator experiment in the same 45° geometry, which we report here. It quickly became apparent that the TTDB model of Ref. [4] gave much too large a prediction for the measured yield. This motivated us to develop an improved model for TTDB which we also report here.

The TTDB model of Ref. [4] was not a rigorous treatment of the effect. It was developed through simple analogy arguments based on the thick-target single bremsstrahlung (TTSB) photon distribution, rather than by a direct integration of the thin-target double bremsstrahlung cross section over the target thickness in a manner equivalent to the derivation of TTSB distribution. Furthermore, the model did not correct for electron backscattering out of the target and could only correct in an average way for photon attenuation.

In the present paper, we present a model for TTDB which integrates over the target thickness the theoretical thin-target DB cross section, doubly differential in photon energy and angle, and corrects for electron backscattering and photon attenuation. Both the model of Ref. 4 and the present model account for the possibility of the incoherent emission of two single bremsstrahlung photons by two separate interactions of the electron within the target. However, the present model uses a more accurate tabulation of the single bremsstrahlung cross section [11] to compute the effect than did the previous model.

The prediction of the model is compared to coincidence yields obtained for thick targets of C, Al, Ag, and Ta bombarded by a 70-keV electron beam for photons detected at ±45° to the incident-beam direction. The present model is found to agree well with the experimental thick-target two-photon yield and to predict a yield which is substantially less than that predicted by the earlier model of Ref. [4]. Of course, the good agreement previously found between the model of Ref. [4] and the ^{109}Cd data of Ref. [6] has now become a puzzle. We believe that we have resolved the puzzle by finding a significant component of ^{113m}Cd in the original source. A reanalysis of the original ^{109}Cd data and a comparison with the present TTDB model is planned to be presented in a separate publication.

II. EXPERIMENTAL DETAILS

Bombarding electrons are provided by an electron accelerator tuned to a nominal energy of 70 keV. Targets are positioned perpendicular to the incident beam within a small scattering chamber which doubles as a Faraday cup for charge collection. The targets are foils of C, Al, Ag, and Ta of around 20–30 mg/cm^2 thickness, which is thick enough to stop 70-keV electrons, and thin enough to effectively transmit the emitted photons. The electron-beam intensity is held at approximately 0.1 nA, which optimizes the ratio of real to accidental coincidences.

The experimental setup, calibration procedure, and determination of solid angles have been described previously [12]. A schematic diagram of the experimental layout and the electronics is shown in Fig. 1. Photons are detected at ±45° to the incident beam in two collimated, planar HpGe detectors, whose efficiencies have been determined in a separate experiment [13]. The geometry

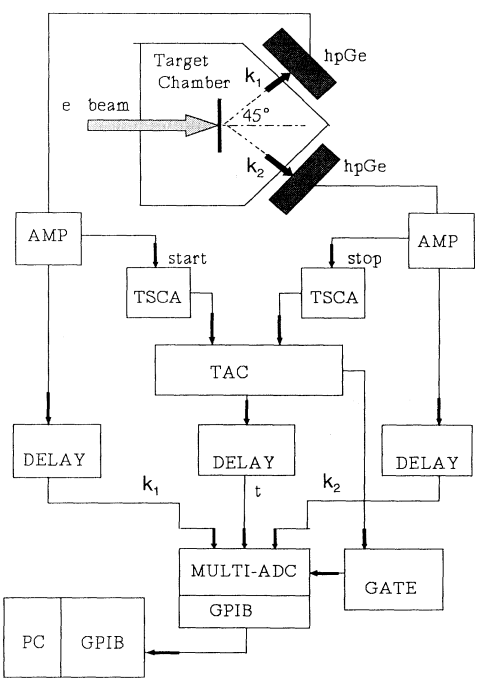

FIG. 1. Schematic diagram of the experimental layout and the electronics. The electron beam from a Cockroft-Walton accelerator enters a small target chamber which serves as a Faraday cup. The photons emitted at ±45° to the beam are detected in hpGe detectors. The data are collected as events consisting of the two-photon energies and the time between them.

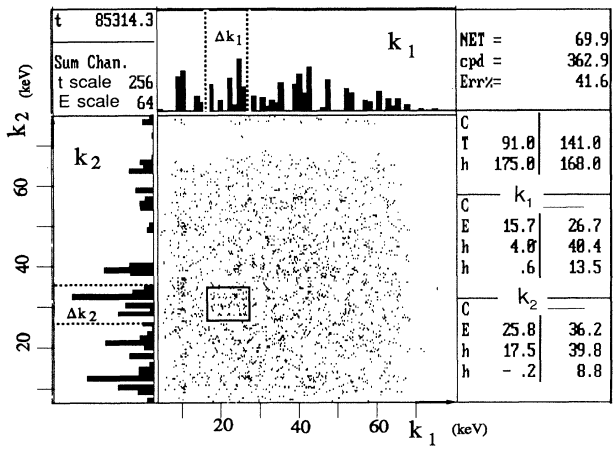

FIG. 2. Printout of a portion of the computer program screen for the data analysis program illustrating the net two-dimensional photon energy event array and several other details described in the text.

was chosen to eliminate cross talk between the detectors and to optimize the solid angles. Individual events consist of the delay time Δt between the two detected photons and their respective energies k_1 and k_2. Software was developed for processing the data to obtain a two-dimensional energy array of the net number of coincident events with the statistical error. To do this, the total events from a run are sorted to produce two energy arrays corresponding to events whose delay times fall inside and outside of the real coincidence timing peak region. A net coincidence energy array is computed by subtraction of the two energy arrays, appropriately normalized.

A typical two-dimensional energy spectrum is shown in Fig. 2. The array of dots is the net events plotted versus increasing photon energy of photon 1 horizontally and photon 2 vertically. The singles spectra are the vertical and horizontal sums of events. The small box encloses a typical two-dimensional energy window. Within the box the net number of counts is shown on the right at 69.9 with a percent error of 41.6. The other information shown on the right refers to counts (h) in selected channels for k_1 or k_2 which are calibrated to energy (E) in keV. The array shown is a four channel sum of the data and the energy window (box) extends from 15.7 to 26.7 keV and from 25.8 to 36.2 keV. Though it is not very clear in this figure, there are points of two shades in the two-dimensional energy spectrum. The darker points are positive, the lighter points are negative. Positive or negative counts can result when the events in the accidental event region are subtracted, properly scaled, from the events within the real event region to form the net spectrum.

III. THEORETICAL CALCULATION

To model two-photon coincident emission in thick targets, two separate, experimentally indistinguishable effects have been considered. The first effect is TTDB, a coherent process in which the two photons are emitted during a *single* interaction of an electron with a single target atom. The second effect is the incoherent emission of two single bremsstrahlung (SBSB) photons by two separate interactions of the electron within the target, or by two different but correlated electrons. The SBSB effect cannot be distinguished from TTDB since the transit time of the electron through the target is of the order of 10^{-15} s, whereas the resolution time of the system is approximately 50 ns.

A. TTDB contribution

An expression for the coherent TTDB yield may be obtained by beginning with the DB photon yield for a thin target, which is given by

$$Y_{\text{thin}}=\frac{N_c}{N_e}=\frac{d^4\sigma}{dk_1dk_2d\Omega_1d\Omega_2}\times t\Delta k_1\Delta\Omega_1\epsilon_1(k_1)\Delta k_2\Delta\Omega_2\epsilon_2(k_2)=C\frac{d^4\sigma}{dk_1dk_2d\Omega_1d\Omega_2}t\Delta k_1\Delta k_2\ , \tag{1}$$

where t is the target thickness, $\Delta k_{1,2}$ are the photon energy windows, $\Delta\Omega_{1,2}$ are the detector solid angles, $\epsilon_{1,2}$ are the energy-dependent detector efficiencies, and C is the product of the detector solid angles and efficiencies. The theoretical DB cross section has been evaluated by performing a numerical integration over the unobserved electron of the complicated formula for the cross-section differential in the two-photon energies and angles and the electron angles and given as Eq. (3) by Smirnov in Ref. [3].

The thick-target yield, neglecting photon attenuation and electron backscattering, is obtained by integrating the theoretical thin-target DB cross section over the whole range of the effective target thickness, as indicated by Eq. (2),

$$Y_{\text{TTDB}}=C\Delta k_1\Delta k_2\int_0^{t_{\max}}\frac{d^4\sigma}{dk_1dk_2d\Omega_1d\Omega_2}dt\ . \tag{2}$$

To account for electron energy loss within the target material, the integration assumes a continuous slowing-down approximation, where the mean electron energy loss is calculated using Bethe's stopping-power theory. The integration was performed using interpolations of the tabulated values for the electron energy loss of Seltzer and Berger [14]. The maximum value of the electron penetrating range is determined from the incident electron energy and the energies of the two emitted photons. The integral over the target thickness may be written as

$$\int_0^{t_{\max}}dt=\int_{E_0}^{k_1+k_2}\left[-\frac{1}{dE/dt}\right]dE\ , \tag{3}$$

where E is the energy of the electron at the position from which the two photons are emitted, and dE/dt is the electron energy loss per unit thickness.

Photon attenuation has been corrected by using mass attenuation coefficients obtained by interpolating the tabulated data of Storm and Israel [15]. The correction factor used is given by the exponential law for photon attenuation, namely,

$$A(k_1,k_2)=\exp\left[-\frac{\mu(k_1)+\mu(k_2)}{\cos\theta}[t-t'(E)]\right], \quad (4)$$

where μ is the energy-dependent absorption coefficient, θ is the photon emission angle, t is the total target thickness, and t' is the electron penetration distance at which the photons are emitted.

Finally, integration of the cross section over the photon energy window $\Delta k_1 \Delta k_2$ including photon attenuation and electron energy loss gives

$$Y_{\mathrm{TTDB}}=C\int_{E_0}^{k_1+k_2}\left[-\frac{1}{dE/dx}\right]\int_{k_1-\Delta k_1/2}^{k_1+\Delta k_1/2}\int_{k_2-\Delta k_2/2}^{k_2+\Delta k_2/2}\frac{d^4\sigma}{dk_1dk_2d\Omega_1d\Omega_2}A(k_1,k_2)dE\,dk_1dk_2\ . \quad (5)$$

A numerical integration of Eq. (5) is performed by using the method of Gaussian quadratures, which approximates the integral by the sum of its functional values at a chosen set of points, multiplied by appropriate weighting factors [16]. The integration proceeds by first determining the maximum penetration range within a target of atomic number Z that the incident electron may travel while maintaining the capability of producing two coincident photons of energies k_1 and k_2. This requirement is met by choosing a maximum electron energy $E_{\max}$ equal to the incident energy E_0, and a minimum energy of $E_{\min}=k_1+k_2$. After the range is obtained, it is then divided into a selected number of layers, and the energy of the incident electron at the position of each layer E_e, is computed assuming a continuous slowing down of the electron through the target material. The electron range and energy loss are determined by an interpolation of the tabulated data of Seltzer and Berger [14]. The next step is to determine the TTDB yield within each separate layer, which is done by integrating, for each value of E_e, the doubly differential DB cross section over a range of possible emitted photon energies. The DB cross section is determined by integrating the fully differential cross section of Ref. [3] over the angles of the unobserved scattered electron. For each value of E_e, an integration over a range of possible k_1 values is performed, where for each value of k_1, the cross section is integrated over a set of k_2 values. The results for the separate layers are then summed, and a total yield is computed.

B. Incoherent SBSB contribution

For the case of a thin target, the probability of the incoherent SBSB interaction is much smaller than the probability for DB, and may thus be ignored. In a thick target, however, this process may contribute significantly to the two-photon yield. The contribution from the incoherent effect is evaluated by assuming a continuous slowing-down approximation for the electron energy loss with target depth. An incident electron of energy E_0 loses energy as it penetrates the target. At some position within the target the electron, whose energy has decreased to some value E, interacts with an atom and emits a photon. At some time Δt later, the electron, now of energy E', undergoes a second interaction and emits the second photon. The delay time Δt is short enough that the detected photons are indistinguishable from those due to DB. It is assumed that as the electron travels through the target, it remains essentially undeflected, and thus continues to move in a straight line of motion. To simulate this process, an integration of the product of the theoretical SB cross sections evaluated at the points of photon emission is performed. The theoretical SB cross section is obtained from the tabulation of Kissel, Quarles, and Pratt [11]. The first photon is integrated over the whole range from the front surface of the target to the maximum depth that the electron penetrates. The second photon is integrated from the position at which the first photon is produced to the maximum depth. The yield obtained from the incoherent effect is therefore given by

$$Y_{\mathrm{SBSB}}=C\int_{E_0}^{k_1+k_2}\left[-\frac{1}{dE/dx}\right]\int_{E-k_1}^{k_2}\left[-\frac{1}{dE'/dx}\right]\int_{k_1-\Delta k_1/2}^{k_1+\Delta k_1/2}\int_{k_2-\Delta k_2/2}^{k_2+\Delta k_2/2}S(E,k_1)S(E',k_2)A(k_1)\times A(k_2)dE\,dE'dk_1dk_2\ , \quad (6)$$

where $S(E,k)$ is the differential cross section for single bremsstrahlung: $d\sigma/d\Omega dk$ and $A(k)$ is the attenuation factor of Eq. (4) for a single photon.

C. Relative weight of TTDB and SBSB processes

Since the models for TTDB and incoherent SBSB determine the yields from these two processes separately, it is assumed that a single incident electron may produce one or the other of the two effects, but not both. The probability for either of the processes to occur regardless of whether a photon is detected depends in an unknown way on the total cross section, target atomic number and thickness, incident electron energy, photon energies or experimental geometry, etc. Therefore, to evaluate the total yield due to the combination of the two effects, a relative weight parameter has been used to fit the combination of the predictions from the two processes to the experimental data. The total yield can be described as

$$Y_{\mathrm{total}}=w_{\mathrm{TTDB}}Y_{\mathrm{TTDB}}+w_{\mathrm{SBSB}}Y_{\mathrm{SBSB}}\ ,$$
$$w_{\mathrm{TTDB}}+w_{SBSB}=1\ , \quad (7)$$

where w_{TTDB} and w_{SBSB} are the normalized weights for the two processes. By varying separately the corresponding weights, a curve for the total yield can be obtained which fits the experimental data well. The weights, which have been assumed here to depend only on the Z of the target, reflect the total probability for one or the other of the exclusive processes to occur when an electron is incident on the target whether or not the photons are detected in the specific geometry of the experiment.

IV. RESULTS

A. Comparison of the present model with the model of Ref. [4]

A comparison of the prediction of the present TTDB model with that of Ref. [4] is shown in Fig. 3 for the cases of C and Ta. As can be seen, the present model predicts a yield that is several orders of magnitude less than that predicted by the earlier model. The difference is larger for the lower Z case. The present model is based on an integration of the thin-target DB cross section that is differential in both photon energies and angles. Thus, if the thin-target DB cross section is correct, we could not expect to get a contribution from TTDB in a low-Z thick target, such as Mylar, that is sufficient to explain the DB cross section reported in Ref. [2]. Clearly some other explanation for that discrepancy must be sought.

B. Experimental yields

The experimental photon yield is determined by the net number of counts and the total charge number,

$$Y_{\mathrm{exp}}=\frac{N_c}{N_e}=\frac{N_c(k_1,k_2,\Delta k_1,\Delta k_2)}{QR} . \tag{8}$$

Here, N_c is the net number of counts, N_e is the charge number for the electrons which induce the two-photon emission, and Q is the total charge. To correct for electron backscattering, a correction factor R, which depends on the energy of the radiated photons, is used [17], namely,

$$R=\frac{1-\eta}{1-\eta\lambda^2}, \quad \lambda=\frac{k_1+k_2}{E_0} . \tag{9}$$

Here, η is the electron-backscattering coefficient for normal electron incidence on massive homogeneous targets, taken from Ref. [18]. This correction is applied to the data as a photon energy-dependent scale factor correction to the total incident charge rather than being incorporated into the model.

The results are displayed in Figs. 4–9. Each figure shows the two-photon yield versus photon energy k_2 varying from 5 to 55 keV, with k_1 held fixed. Figures 4 and 5 display the results for C and Al, respectively, with $k_1=10$ keV. The results for Ag and Ta are shown in Figs. 6–9, with $k_1=10$ keV in Figs. 6 and 7, and $k_1=20$ keV in Figs. 8 and 9. The photon energy window widths were chosen as 10 keV in order to obtain acceptable statistical errors, and the midpoints of the windows were varied to acquire different combinations of two-photon emission. The error bars represent the one standard deviation statistical error in the yield. The systematic errors in target thickness, charge collection, solid angle, and detector efficiency are small compared to the statistical error, and subtraction of a target-out background was found not to be necessary since spectra collected with no target present displayed no measurable two-photon effect.

In each figure, the dashed line gives the TTDB yield predicted by the present model. The TTDB yield has been multiplied by the Elwert factor which tends to correct the Z dependence of the first Born approximation, and which has traditionally been used as a correction for single bremsstrahlung [19]. The dot-dashed line is the prediction of the present model for incoherent SBSB. The solid line is the weighted average obtained by multiplying each model prediction by a value of the corresponding parameter, w_{TTDB} or w_{SBSB}, which gives a good fit of the combination of the two models to the data.

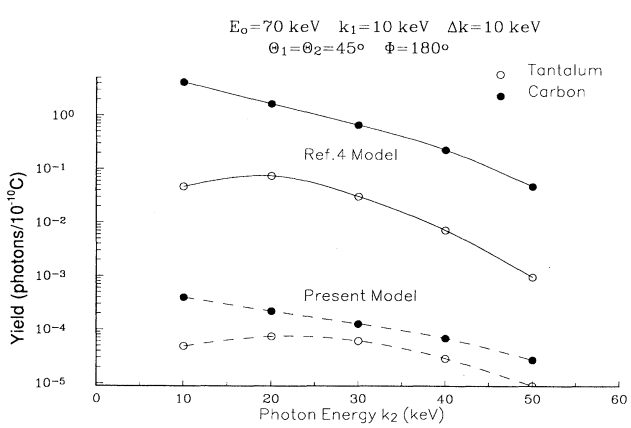

FIG. 3. Comparison of the present model for TTDB with the model of Ref. [4] for C and Ta targets. Both models include photon attenuation.

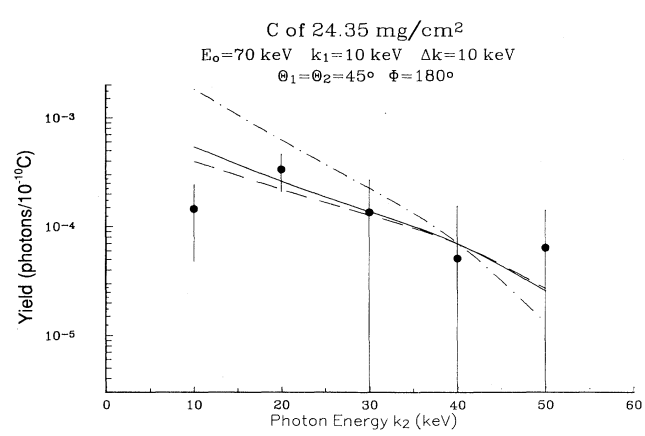

FIG. 4. The two-photon yield for C target with thickness of 24.35 mg/cm^2 vs photon energy k_2. k_1 is fixed at 10 keV. The dashed line is the TTDB yield from the present model. The dot-dashed line is the SBSB yield from the present model. The solid line is a weighted average with $w_{\mathrm{TTDB}}=0.9$ and $w_{\mathrm{SBSB}}=0.1$.

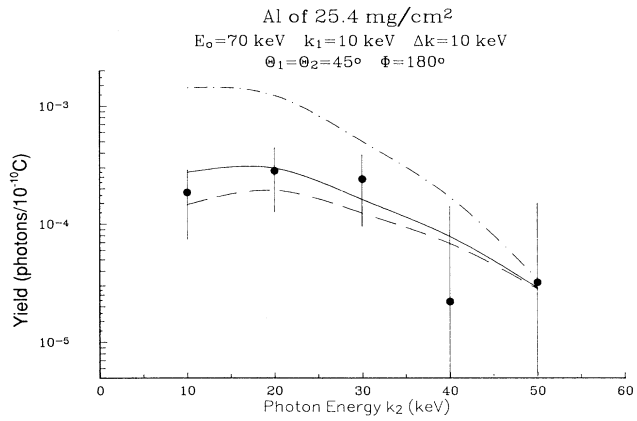

FIG. 5. Same as Fig. 4 for Al of thickness 25.4 mg/cm^2.

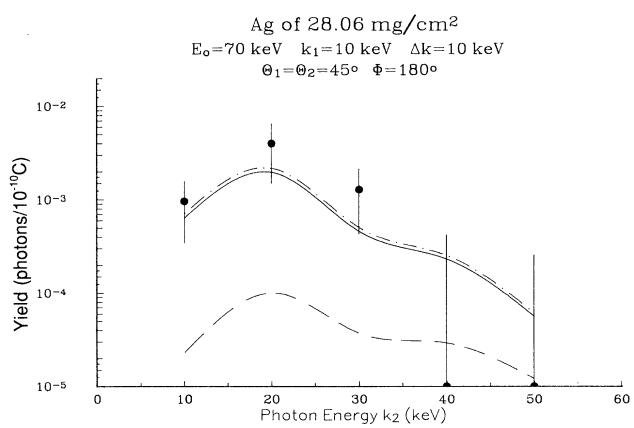

FIG. 6. The two-photon yield for Ag target with thickness of 28.06 mg/cm^2 vs photon energy k_2. k_1 is fixed at 10 keV. The dashed line is the TTDB yield from the present model. The dot-dashed line is the SBSB yield from the present model. The solid line is a weighted average with $w_{\mathrm{TTDB}}=0.1$ and $w_{\mathrm{SBSB}}=0.9$.

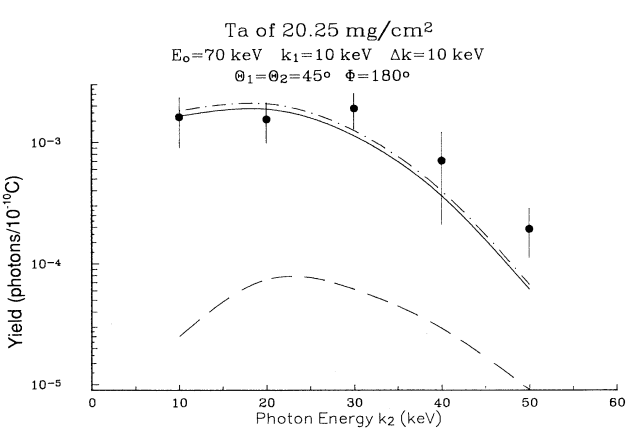

FIG. 7. Same as Fig. 6 for Ta of thickness 20.25 mg/cm^2.

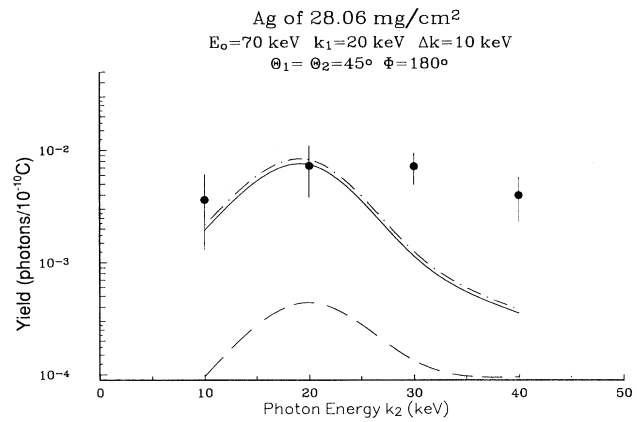

FIG. 8. The two-photon yield for Ag target with thickness of 28.06 mg/cm^2 vs photon energy k_2. k_1 is fixed at 20 keV. The dashed line is the TTDB yield from the present model. The dot-dashed line is the SBSB yield from the present model. The solid line is a weighted average with $w_{\mathrm{TTDB}}=0.1$ and $w_{\mathrm{SBSB}}=0.9$.

For the low-Z targets of C and Al shown in Figs. 4 and 5, the data are systematically lower than the prediction of the SBSB model and tend to agree better with the prediction of the TTDB model both in magnitude and in photon energy dependence. Selecting weights of $w_{\mathrm{TTDB}}=0.9$ and $w_{\mathrm{SBSB}}=0.1$ gives a weighted average that agrees well with the data. Comparison of the TTDB line with the weighted average line suggests that any weight factor with w_{SBSB} less than 10% would fit the data. For both C and Al, the model reproduces well the energy dependence displayed by the data, and the prediction agrees with the data to within one standard deviation of error, with the exception of the point at $k_2=10$ keV for C.

For the higher-Z targets of Ag and Ta displayed in Figs. 6–9, the data agree better with the SBSB model in both magnitude and energy dependence. For the sufficiently high Z, we would expect SBSB to dominate over TTDB from the Z^4 dependence of SBSB versus the Z^2 of TTDB, and the data support this expectation.

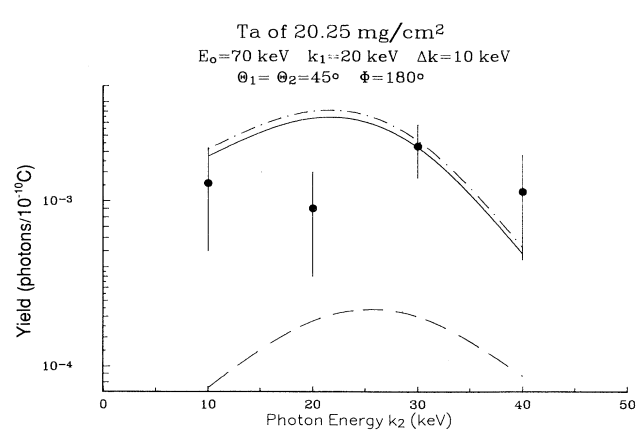

FIG. 9. Same as Fig. 8 for Ta of thickness 20.25 mg/cm^2.

Selecting values of $w_{\mathrm{TTDB}}=0.1$ and $w_{SBSB}=0.9$ gives generally good agreement, except for several points, between the shape of the predicted curve and the energy dependence displayed by the data. Of course, a value of w_{TTDB} less than 10% would also fit well as can be seen by comparing the weighted average (solid line) with the SBSB model (dot-dashed line).

For k_1 fixed at 10 keV for both Ag and Ta in Figs. 6 and 7, there is a good agreement between both the magnitude and the energy dependence of the model and the data. For $k_1=20$ keV shown in Figs. 8 and 9, the agreement is generally not as good in detail. For Ag (Fig. 8), the two data points at higher k_2 are significantly higher than the model. For Ta (Fig. 9), the agreement is good except for the point at 20 keV.

A possible reason for some discrepancies observed in the high-Z data of Ag and Ta might be the fact that the model does not include the emission of a characteristic x ray in coincidence with a SB photon. The existence of K x rays between 21 and 25 keV for Ag could account for some of the enhancement in the yield for the case of $k_1=20$ keV shown in Fig. 8. There could also be a similar effect for the 10 keV points of Ta since this point includes L x rays. However, in this case no significant enhancement is observed.

V. CONCLUSIONS

Measurements of the two-photon yield for 70 keV electrons on thick targets of C, Al, Ag, and Ta are reported. The yield is determined for photons emitted at $\pm 45°$ to the incident electron beam. The experimental yields are several orders of magnitude less than the prediction of the simple model of Ref. [4]. A more rigorous model of both coherent TTDB and incoherent SBSB has been developed that compares well with the experimental yields when the two competing processes are selectively weighted. The data are consistent with TTDB being the dominant process for low Z of C and Al, while the SBSB process is dominant for the higher Z of Ag and Ta.

There are two effects that have not been included in the present model that may need to be considered in the future. First, the model does not integrate over the solid angles subtended by the two-photon detectors. It has been assumed that the yield would vary little over these solid angles. While this appears to be reasonable for the 45° geometry, it may not be so appropriate for different angles where the cross sections in the integrals may change more rapidly. Related to this is the assumption that the electron continues to travel in the forward direction. In a separate study, we found that in single bremsstrahlung the most probable direction for the electron is forward even when the angle of emission of the photon is 45°. If the model included the additional integrals over the detector solid angles, one could also include the effect of the multiple scattering that spreads the electron beam over an average angular range as it penetrates the target and loses energy. The second effect not included in the current model is the multiple emission of characteristic x rays as the electron penetrates the target and loses energy. It is clear that there can be an average multiplicity of x rays, limited by the ratio of the total available energy to the atomic binding energy. This has been suggested above as an explanation for the enhancement seen in the Ag data when one photon window includes the Ag K x ray. However, it is not clear how to include the ionization effect, with its much larger cross section, into the present model unless one undertakes a full Monte Carlo model which can handle processes with very different probabilities.

As a consequence of the more rigorous model and the results presented here, the conclusions based on the previous model of Ref. [4] should be reexamined. First, it does not any longer seem plausible that thick-target double bremsstrahlung in the Mylar windows is the explanation for the much larger DB cross section measured by Ref. [2]. The agreement obtained in Ref. [6] between the data from ^{109}Cd radiating thick targets and the prediction of the earlier TTDB model requires further explanation. Recently, in a separate investigation of the β-decay spectrum in a Si(Li) detector it was discovered that the ^{109}Cd source used has a significant component of ^{113m}Cd. This isotope has a beta decay spectrum with an electron endpoint energy of 585 keV. Thus there was a very substantial component of electrons with energies greater then the 84-keV conversion electron energy assumed. A reconsideration of the ^{109}Cd–^{113m}Cd data is currently underway.

ACKNOWLEDGMENTS

This research was supported by the Welch Foundation and the TCU Research Fund.

[1] W. Heitler and L. Nordheim, Physica **1**, 1059 (1934).
[2] J. C. Altman and C. A. Quarles, Phys. Rev. A **31**, 2744 (1985); Nucl. Instrum. Methods Phys. Res. A **240**, 538 (1985).
[3] A. I. Smirnov, Yad. Fiz. **25**, 1030 (1977) [Sov. J. Nucl. Phys. **25(5)**, 548 (1977)].
[4] H. E. Lehtihet and C. A. Quarles, Phys. Rev. A **39**, 4274 (1989).
[5] R. Ambrose, D. L. Kahler, H. E. Lehtihet, and C. A. Quarles, Nucl. Instrum. Methods Phys. Res. B **56/57**, 327 (1991).
[6] H. E. Lehtihet and C. A. Quarles, Nucl. Instrum. Methods Phys. Res. A **280**, 202 (1989).
[7] D. K. Kahler, J. Liu, and C. A. Quarles, Phys. Rev. Lett. **68**, 1690 (1992).
[8] V. Veniard, A. Maquet, and M. Gavrila, Phys. Rev. A **35**, 448 (1987).
[9] J. Scofield (private communication).
[10] V. Florescu (private communication).
[11] L. Kissel, C. A. Quarles, and R. H. Pratt, At. Data Nucl. Data Tables **28**, 381 (1983).
[12] C. A. Quarles, H. E. Lehtihet, D. J. Lawrence, and D. L. Kahler, Nucl. Instrum. Methods Phys. Res. B **56/57**, 184 (1991).

[13] J. C. Altman, R. Ambrose, C. A. Quarles, and G. Westbrook, Nucl. Instrum. Methods Phys. Res. B **24/25**, 1028 (1987).

[14] S. M. Seltzer and M. J. Berger, *Tables of Energy Losses and Ranges of Electrons and Positrons,* NASA Special Publication No. 3012 (NASA, Greenbelt, MD, 1964).

[15] E. Storm and H. I. Israel, Nucl. Data Tables A **7**, 565 (1970).

[16] W. H. Press, B. P. Flannery, S. A. Teukolsky, and W. T. Vetterling, *Numerical Recipes, The Art of Scientific Computing* (Cambridge University Press, Cambridge, England, 1986).

[17] E. Storm, Phys. Rev. A **5**, 2328 (1972).

[18] H. J. August and J. Wernisch, Phys. Status Solidi A **114**, 629 (1989).

[19] H. W. Koch and J. W. Motz, Rev. Mod. Phys. **31**, 920 (1959).